REPORT DOCUMENTATION PAGE

Form Approved
OMB No. 0704-0188

1. REPORT DATE *(DD-MM-YYYY)*	**2. REPORT TYPE**	**3. DATES COVERED** *(From - To)*
27/09/2022	Conference Presentation	Sep, 2021 - Sep, 2022

4. TITLE AND SUBTITLE

Comparison of Operating Atmosphere Impact on La0.7Sr0.3V3.86-x (LSV) Intermediate-Temperature Solid Oxide Fuel Cell Sulfur Tolerance Explored Through Experimental and Modeling Characterization Over Time

5a. CONTRACT NUMBER

5b. GRANT NUMBER

5c. PROGRAM ELEMENT NUMBER

6. AUTHOR(S)

Theodore E. Burye
Talia M. Sebastian

5d. PROJECT NUMBER

5e. TASK NUMBER

5f. WORK UNIT NUMBER

7. PERFORMING ORGANIZATION NAME(S) AND ADDRESS(ES)

US Army CCDC Ground Vehicle Systems Center (GVSC)
Ground Vehicle Power and Mobility (GVPM)
Force Projection Technology (FPT)
6501 E. 11 Mile Road
Warren, MI 48397

8. PERFORMING ORGANIZATION REPORT NUMBER

OPSEC 6922

9. SPONSORING / MONITORING AGENCY NAME(S) AND ADDRESS(ES)

US Army CCDC Ground Vehicle Systems Center (GVSC)
Ground Vehicle Power and Mobility (GVPM)
Force Projection Technology (FPT)
6501 E. 11 Mile Road
Warren, MI 48397

10. SPONSOR/MONITOR'S ACRONYM(S)

11. SPONSOR/MONITOR'S REPORT NUMBER(S)

12. DISTRIBUTION / AVAILABILITY STATEMENT

DISTRIBUTION A. Approved for public release; distribution unlimited. OPSEC #6922

13. SUPPLEMENTARY NOTES

14. ABSTRACT

Solid Oxide Fuel Cells (SOFCs) have the potential to provide clean, secure, and highly efficient sustainable energy for the U.S. Army. SOFCs can use many different reformed hydrocarbon fuels to obtain hydrogen for power generation, which include externally reformed JP-8, or can directly feed alternative fuels scavenged in theater. One long-term problem, specific for the U.S. Army, is sulfur performance degradation, common in most fuel options. JP-8 is not commonly desulfurized, and any scavenged fuel could be contaminated with sulfur. One solution to this problem could be the anode catalyst material, La0.7Sr0.3VO3.86-x (LSV), which has previously demonstrated significant sulfur tolerance at temperatures greater than 700°C. This study further investigates LSVs sulfur tolerance at intermediate temperatures (400-700°C) in hydrogen and methane atmospheres up to 100 hours, where it was observed to be up to 278-287x more tolerant than Ni-YSZ (700°C), believed to be due to electronic/ionic changes occurring during exposure.

15. SUBJECT TERMS

16. SECURITY CLASSIFICATION OF: Available for Public Release			**17. LIMITATION OF ABSTRACT**	**18. NUMBER OF PAGES**	**19a. NAME OF RESPONSIBLE PERSON**
a. REPORT	**b. ABSTRACT**	**c. THIS PAGE**	Same as Report (SAR)	29	Theodore Burye
UNCLS	UNCLAS	UNCLAS			**19b. TELEPHONE NUMBER** *(include area code)* 586-282-3047

Standard Form 298 (Rev. 8-98)
Prescribed by ANSI Std. Z39.18

U.S. ARMY COMBAT CAPABILITIES DEVELOPMENT COMMAND – GROUND VEHICLE SYSTEMS CENTER

Comparison of Operating Atmosphere Impact on $La_{0.7}Sr_{0.3}VO_{3.86-\delta}$ (LSV) Intermediate-Temperature Solid Oxide Fuel Cell Sulfur Tolerance Explored through Experimental and Modeling Characterization over Time

Theodore Burye, PhD

Chemical Engineer

Ground Vehicle Power & Mobility

Talia Marie Sebastian, PhD

Research Chemist

Fuels and Lubricants Branch

25 APR 22

Motivation – SOFC Sulfur Contamination

Fuel Flexibility and Anode Deactivation

- State-of-the-art (Ni/YSZ)
  - Nickel highly active toward electrochemical oxidation of sulfur, leading to sulfur poisoning and deactivation
  - Chemisorption (<50 ppm(v)), Sulfidation (>50 ppm(v))
  - Concentrations as low as 2 ppm(v) can cause irreversible damage.

Material Strategies for Sulfur Tolerance

- Alloying nickel with noble or base metals
- Replacing nickel with base metals or nonmetal electronic conductors
- Replacing with mixed ionic-electronic conductors (i.e., Perovskite Oxides)

Mechanism of Chemisorption:

$$H_2S_{(g)} \leftrightarrow HS_{(ads)} + H_{(g/ads)} \leftrightarrow S_{(ads)} + H_{2(g)}$$

Mechanism of Sulfidation:

$$Ni_{(s)} + H_2S_{(g)} \leftrightarrow NiS_{(s)} + H_{2(g/ads)}$$

$$3Ni_{(s)} + xH_2S_{(g)} \leftrightarrow Ni_3S_{x(s)} + xH_{2(g)}$$

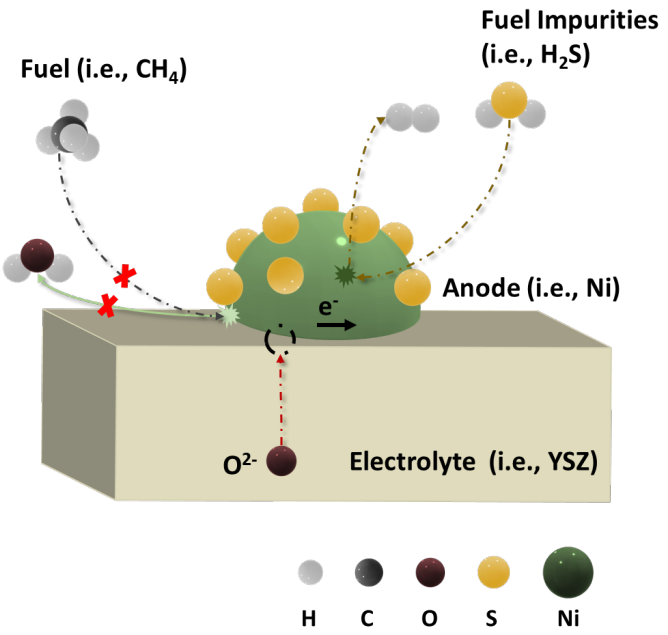

Adapted: DOI: 10.1016/j.jallcom.2017.11.381

Motivation – LSV Anode Catalyst Sulfur Tolerance

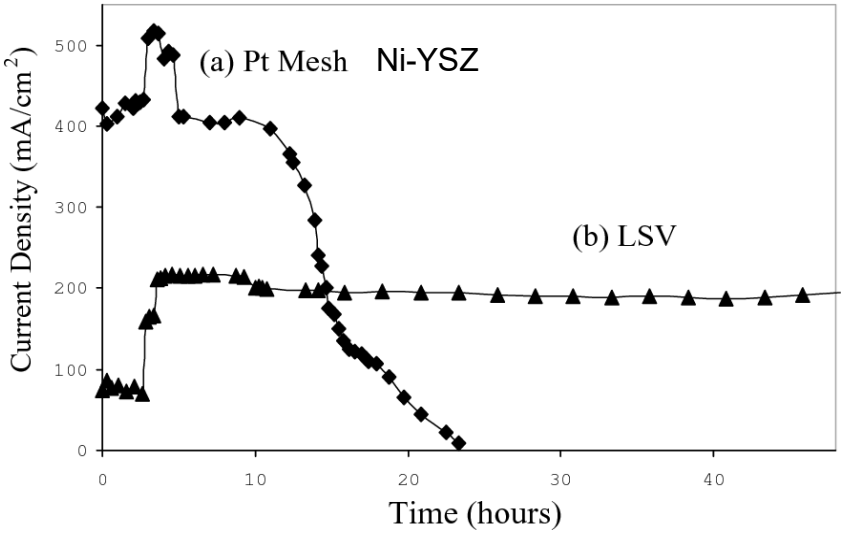

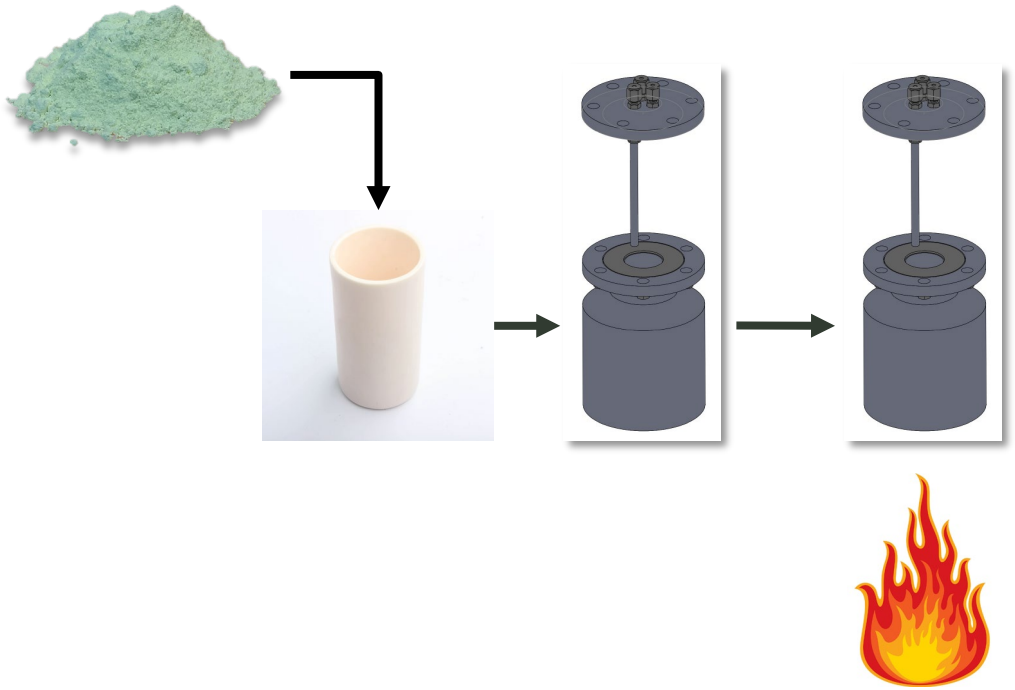

- Literature experimental results show $La_{0.7}Sr_{0.3}V$ oxide (LSV) current-density stability in H_2S contamination
  - 5vol% H_2S – High contaminant concentration
  - 1000C – High temperature for reactions
  - Tested for ~45 hours

- This study experimentally tests LSV powder:
  - Heated under exposure to H_2S
  - Altered atmosphere from H_2 to CH_4
  - Heated up to 100 hours
  - Sulfur amount characterized using EDS post-experimentation
  - LSV structure characterized using XRD post-experimentation
  - Modeling of H_2S and LSV interaction conducted in parallel

Aguilar, J. Power Sources, 135, (2004), 17-24

Experimental Results – Operating Parameters

Gas Pressure = 45 PSI Equivalent Flow Rate = 300 mL/min

H_2S Concentration (ppm)	Balance Gas	Temperature (C)	Time (hours)
30	H_2	400	25-100 hours
30	H_2	500	25-100 hours
30	H_2	700	25-100 hours
30	H_2	400	25-100 hours
300	H_2	500	25-100 hours
300	H_2	600	25-100 hours
300	H_2	700	25-100 hours
30	CH_4	400	25-100 hours
30	CH_4	500	25-100 hours
30	CH_4	600	25-100 hours
30	CH_4	700	25-100 hours

Experimental Results – Adsorption Rates

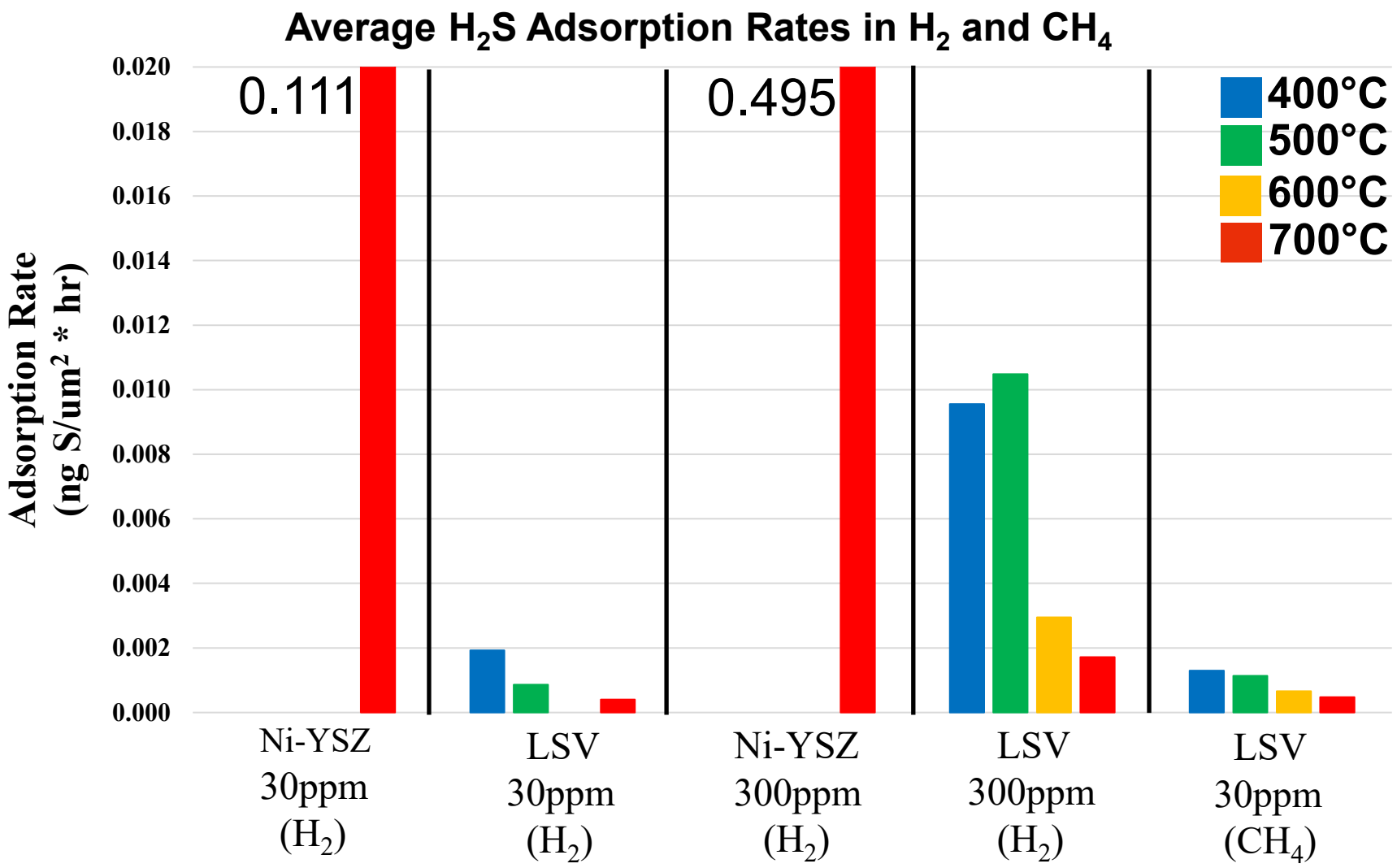

Experimental Results – LSV Raw EDS

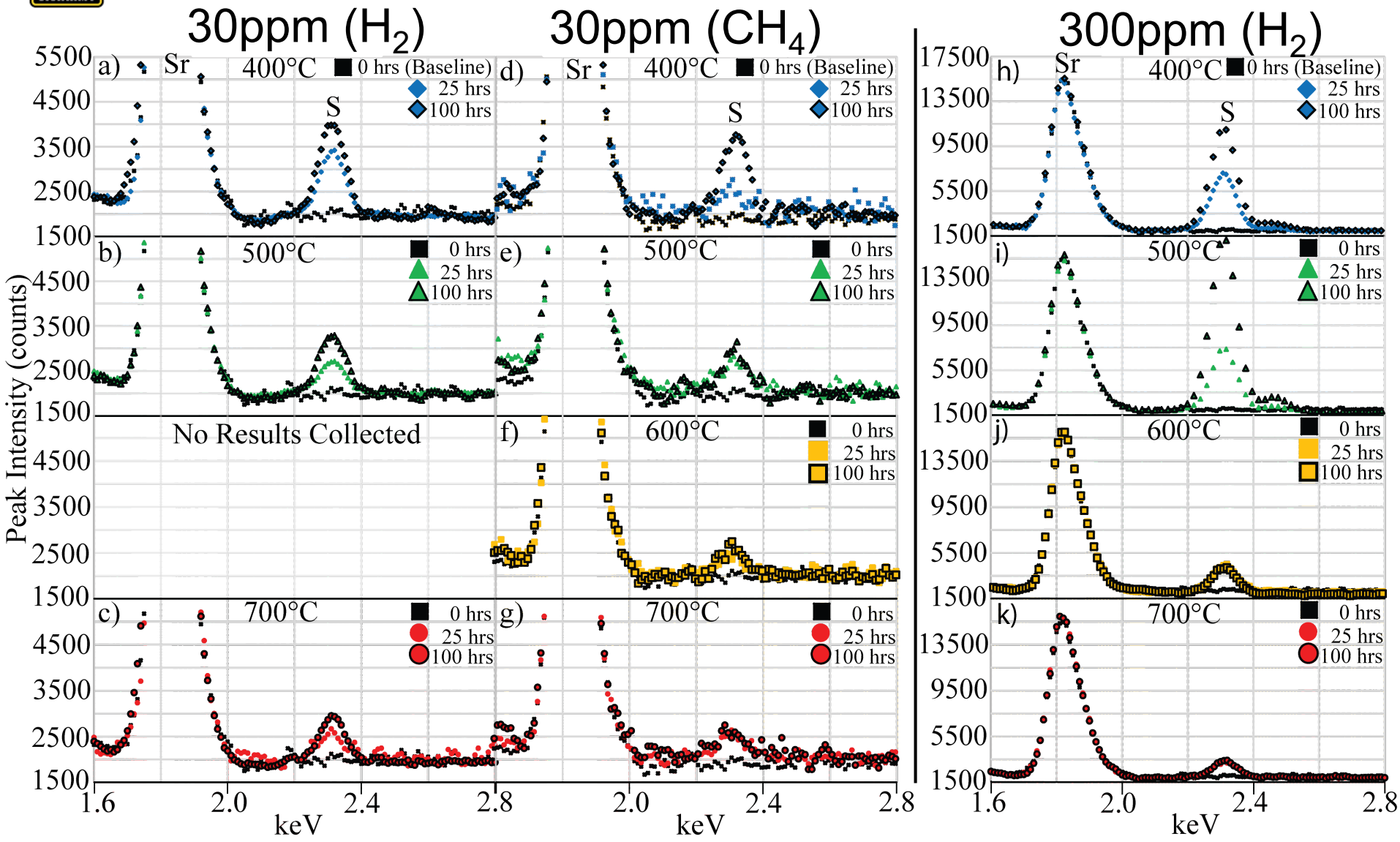

Experimental Results – LSV Agglomerate Size

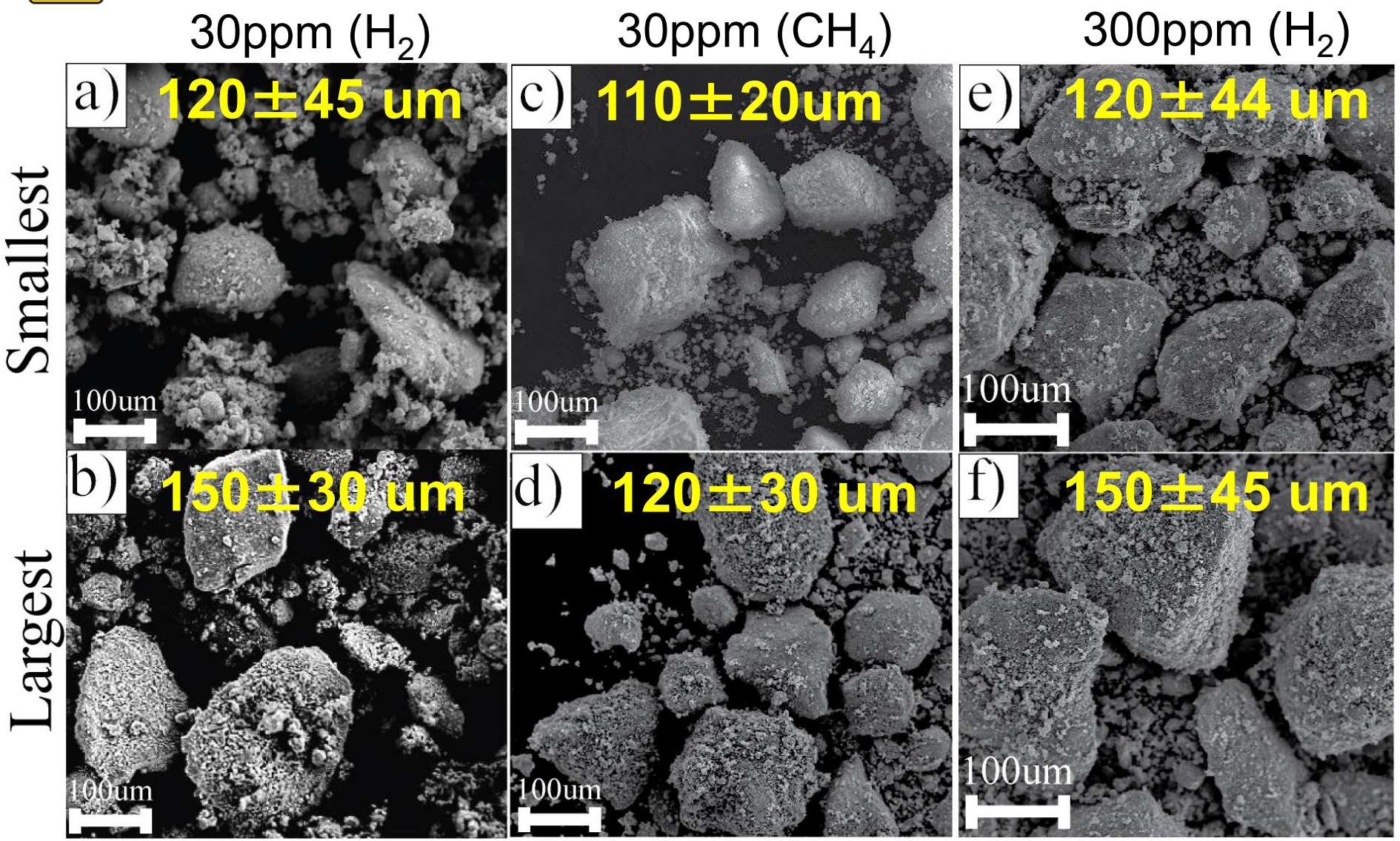

Experimental Results – LSV Raw XRD

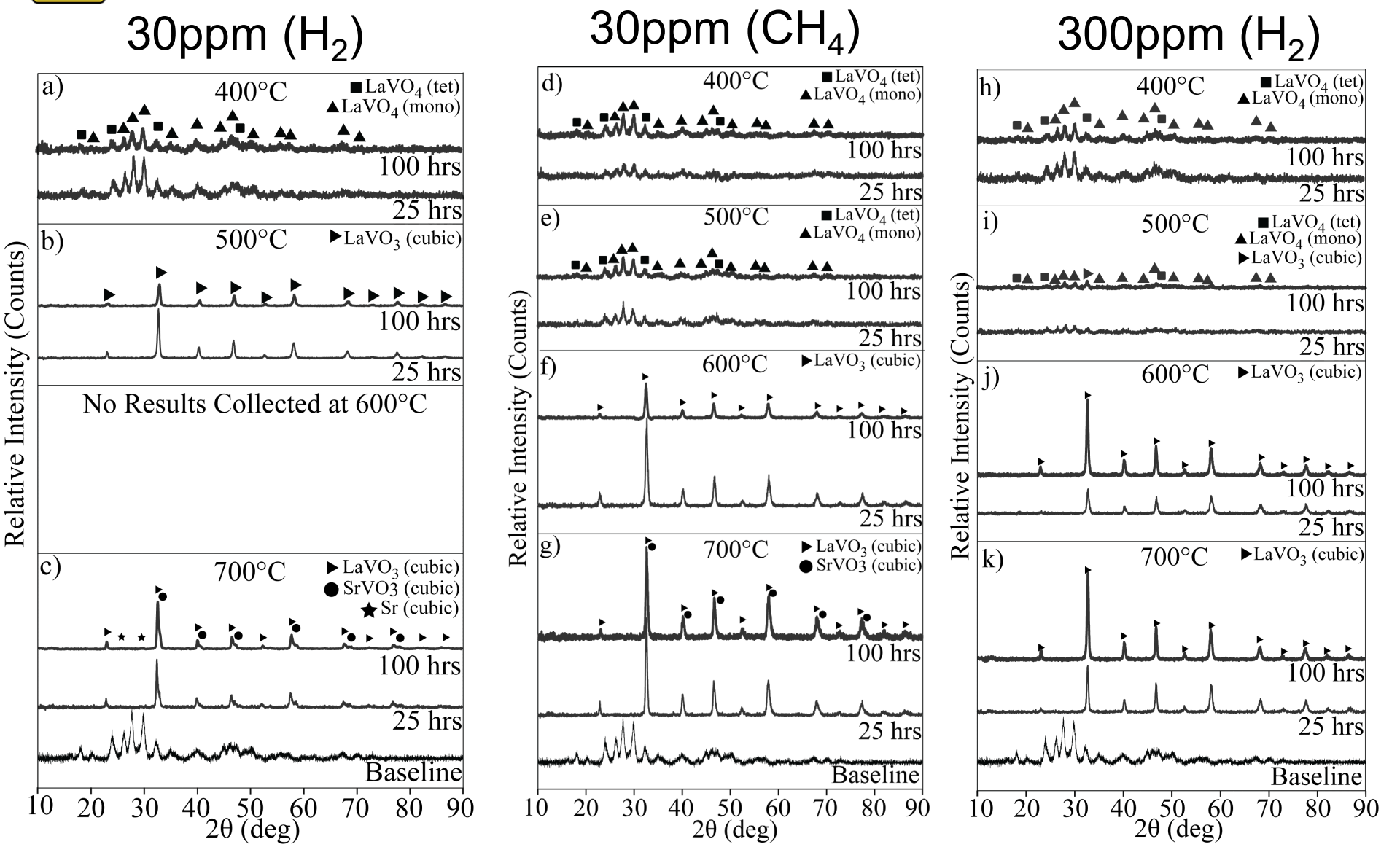

Experimental Results – LSV Activation Energies

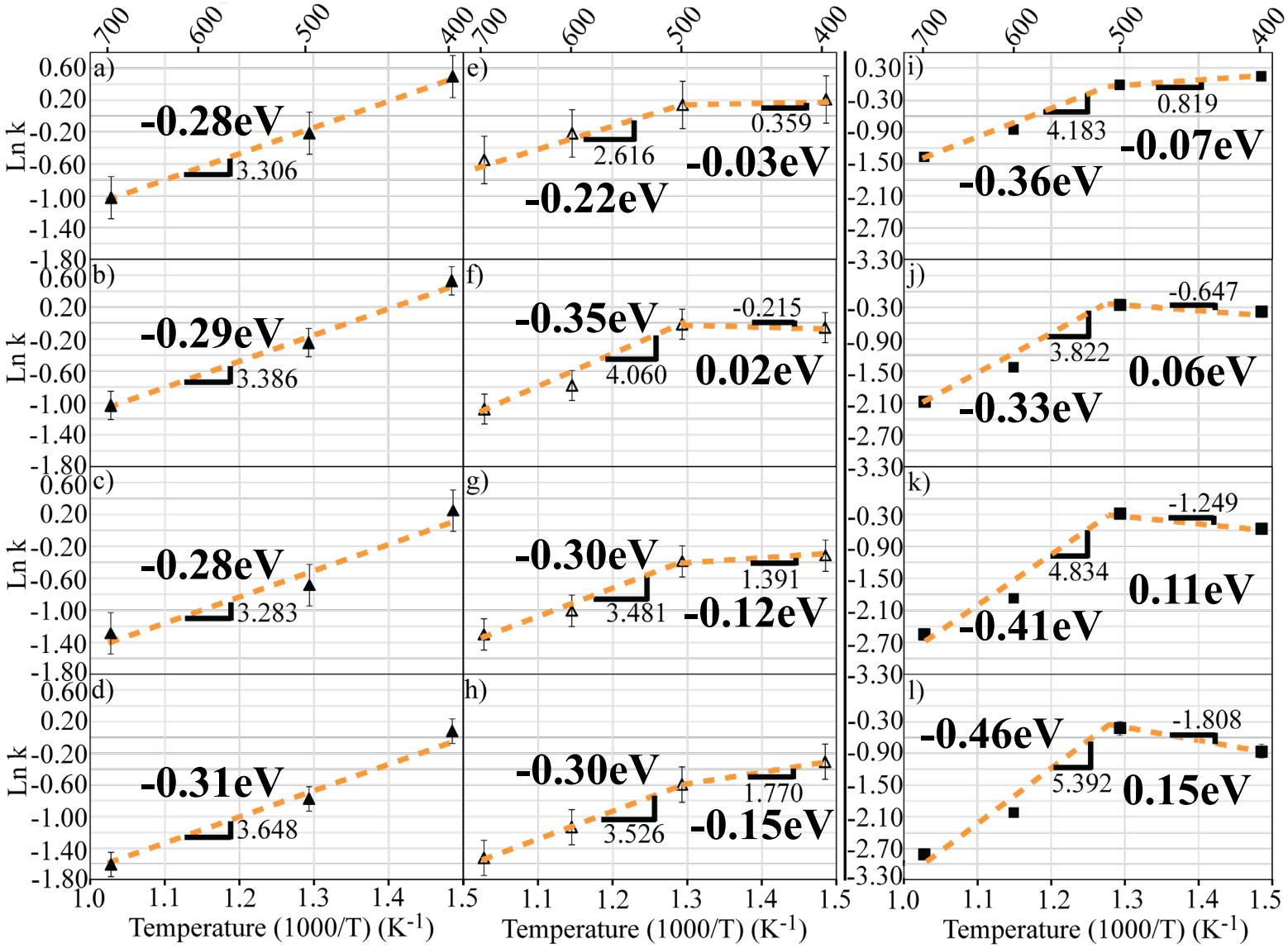

Theoretical Introduction and Literature Review

Density Functional Theory

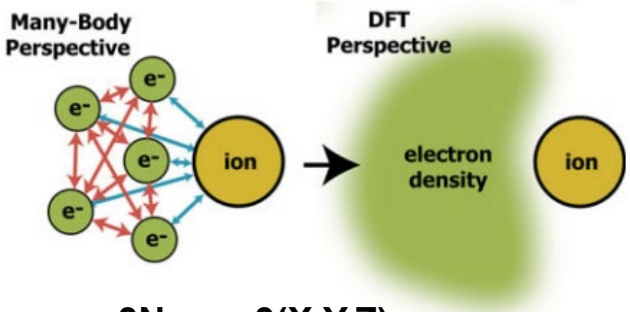

Density Functional Theory in Catalysis

- Atomic structures and surfaces
- Surface active sites and chemical states
- Adsorption and diffusion
- Defects and imperfections
- Electronic structure and distribution

Density Functional Theory Literature Ni/YSZ

- Adsorption of H_2S on nickel surfaces
- Two-step dissociative adsorption reaction
- Favorable reaction process

Density Functional Theory LSV Treatment

- DFT:GGA:PBE:TZP/DZP:Small FC:Normal

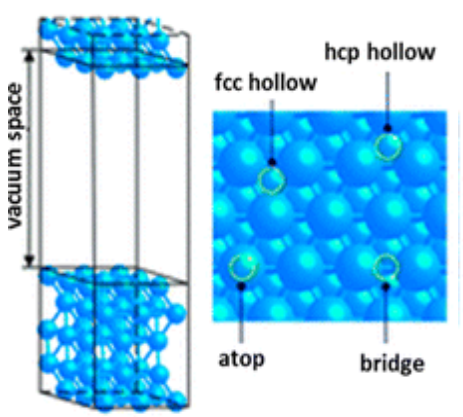

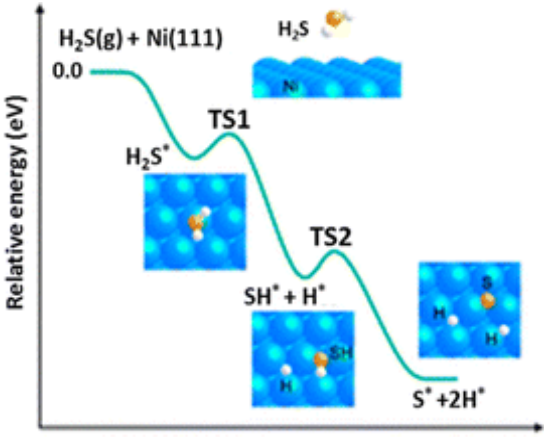

Table 3. Activation Barriers (E_a) and Reaction Energies (ΔE) for the Elementary Steps in a H_2S Dissociative Adsorption Process and Adsorption Energies (E_{ads}) of Sulfur Species (S*, HS*, and H_2S*)[a]

metal	E_{a1}[b]	ΔE_1[b]	E_{a2}[c]	ΔE_2[c]	E_{ads}S*	E_{ads}HS*	$E_{ads}H_2S$*
Pt(111)(93)	0.02	−0.90	0.04	−1.19	5.14	3.00	0.90
Pd(111)(94)	0.37	−1.25	0.04	−0.73	5.15	3.02	0.71
Rh(211)(95)	0.01	−1.50	0.32	−1.50	6.0	3.69	1.00
Ni(100)(88)	0.29	−1.56	0.45	−1.05	5.96	3.72	0.83
Ni(111)(88)	0.15	−0.98	0.11	−0.86	5.14	2.95	0.67

[a] All values in eV.
[b] E_{a1} and ΔE_1 correspond to $H_2S^* \rightarrow HS^* + H^*$.
[c] E_{a2} and ΔE_2 correspond to $HS^* \rightarrow H^* + S^*$.

DOI:10.1021/acs.chemrev.6b00284

Material Introduction and Background

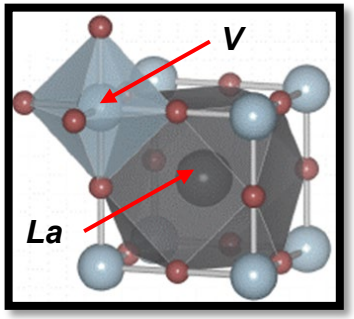

DOI:10.1103/PhysRevB.89.134103

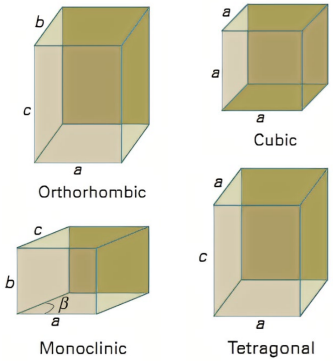

Lanthanum Vanadate ($LaVO_3$) - Reduced

- Orthorhombic: stable (Pnma)
  - a = 5.677 Å, b = 7.942 Å, c = 5.591 Å
  - α = 90.053° , β = 90.115° , γ = 90.003°
- Cubic: metastable ($Pm\bar{3}m$)
  - a = 3.950 Å, b = 3.950 Å, c = 3.950 Å
  - α = 90.000° , β = 90.000° , γ = 90.000°
  - Decomposes to orthorhombic

Lanthanum Orthovanadate ($LaVO_4$) - Oxidized

- Tetragonal: stable ($I4_1/amd$)
  - a = 6.268 Å, b = 6.268 Å, c = 6.268 Å
  - α = 106.091° , β = 106.091° , γ = 116.466°
- Monoclinic: metastable ($P2_1/c$)
  - a = 7.353 Å, b = 6.804 Å, c = 8.463 Å
  - α = 54.455° , β = 90.000° , γ = 90.000°
  - Decomposes to tetragonal

Lanthanum Vanadate ($LaVO_3$) - Reduced

- Reduced structure V^{3+}
- Expected conductor (no bandgap), yet Mott Insulator (1.08 eV bandgap, indirect) between bands of like character (d)
- Partially filled d-orbitals of B-site (V $3d^2$) experience strong electron-electron interactions, preventing conduction

Lanthanum Orthovanadate ($LaVO_4$) – Oxidized

- Oxidized structure V^{5+}
- Insulator (3.50 eV bandgap, indirect)
- Vacant d-orbitals of B-site (V $3d^0$)

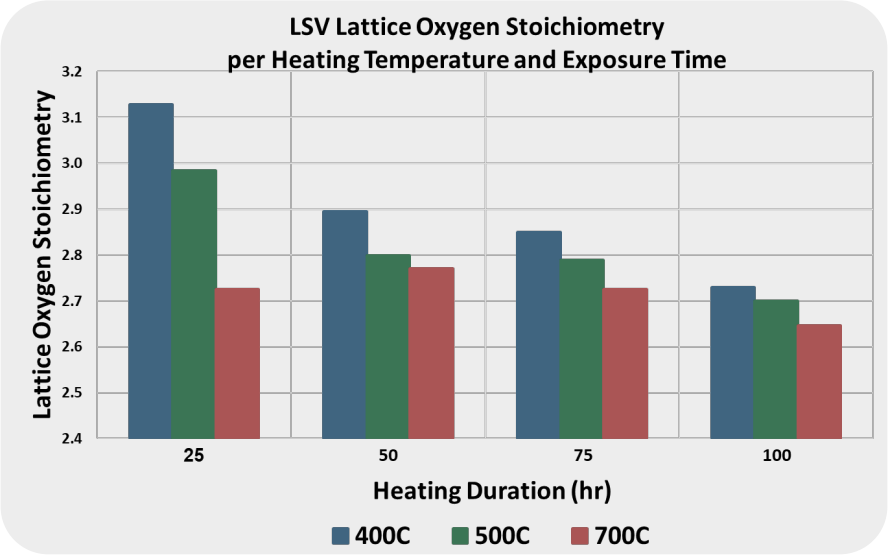

$LSV_{reduced}$ Surface Study

LSV Surface Structures

>50 structures with 0 eV above Hull

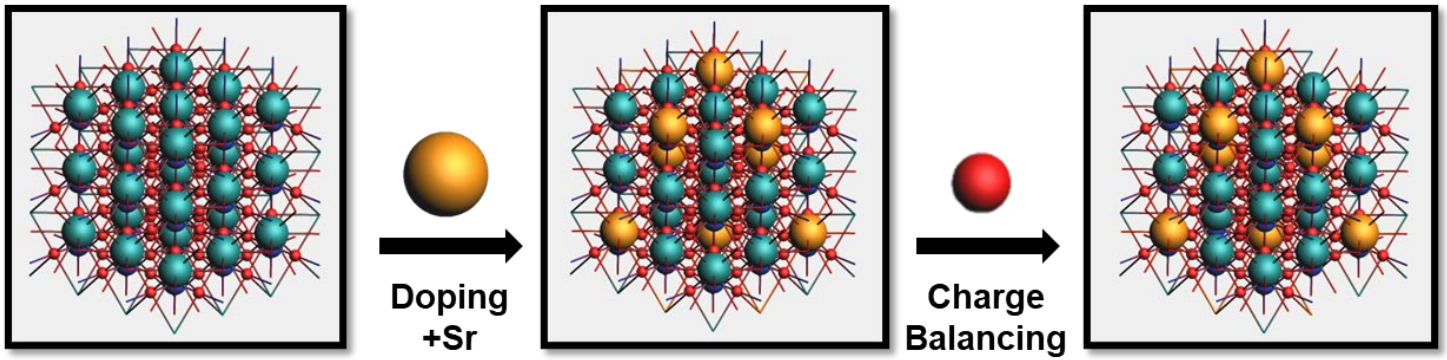

Cubic $LaVO_3$ → Cubic $La_{0.7}Sr_{0.3}VO_3$ → Cubic $La_{0.7}Sr_{0.3}VO_{2.95}$

O: [He] $2s^2 2p^4$
V: [Ar] $4s^2 3d^3$
La: [Xe] $6s^2 5d^1$
Sr: [Kr] $5s^2$

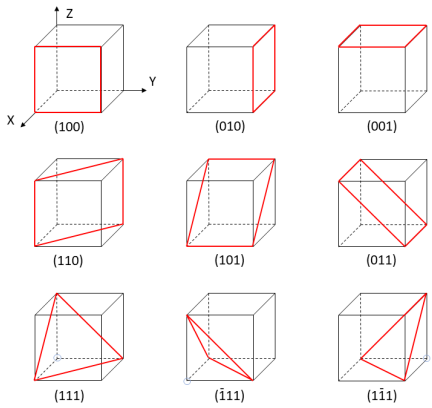

~lowest energy surface (001)
~nonsymmetric/polar

DFT - GGA:PBE:TZP:SFC:Normal

Relaxed Pseudo-cubic $La_{0.7}Sr_{0.3}VO_{2.95}$

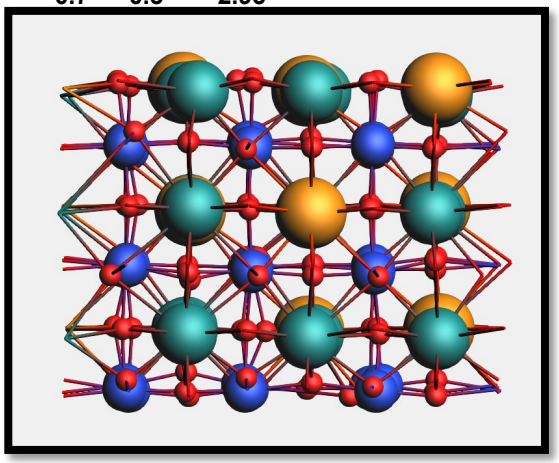

H_2S

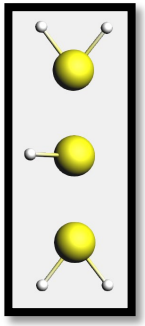

top (t)
bridge (b)
hollow (h)
pseudo-hollow (ph)

La/SrO Termination

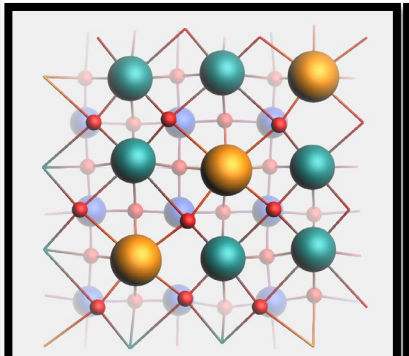

VO Termination

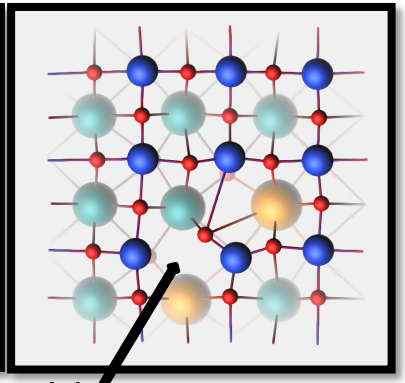

**vacancy (v)*

$LSV_{reduced}/H_2S$ Adsorption Study

Adsorption Products on La/Sr Termination

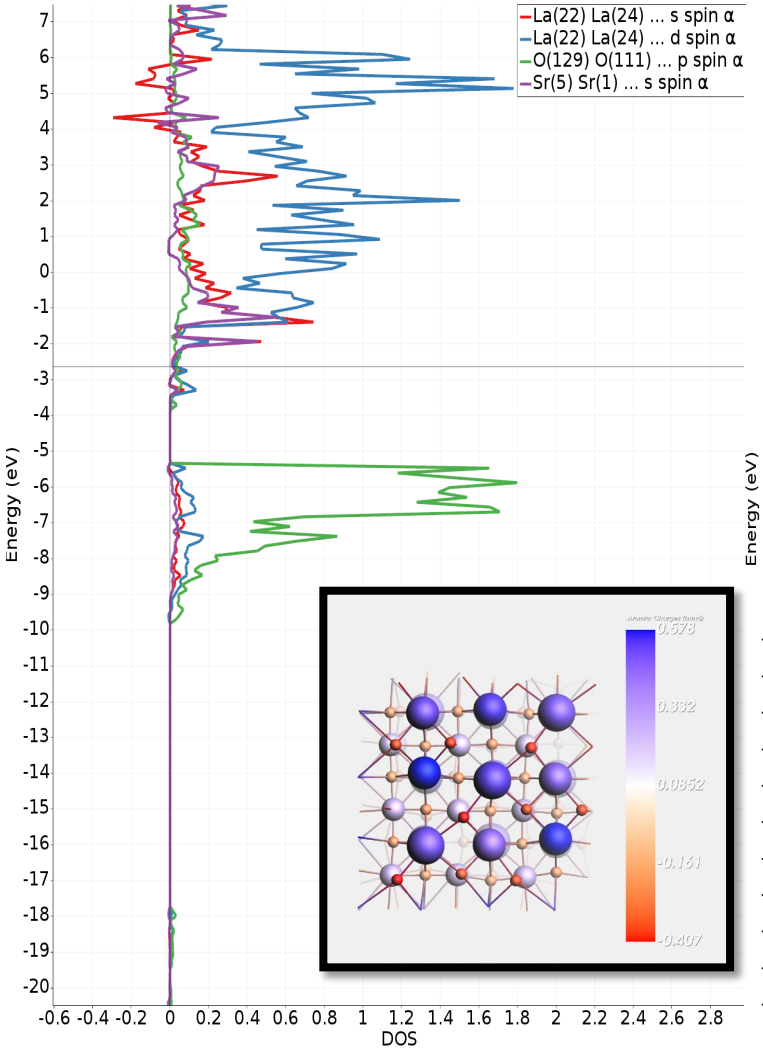

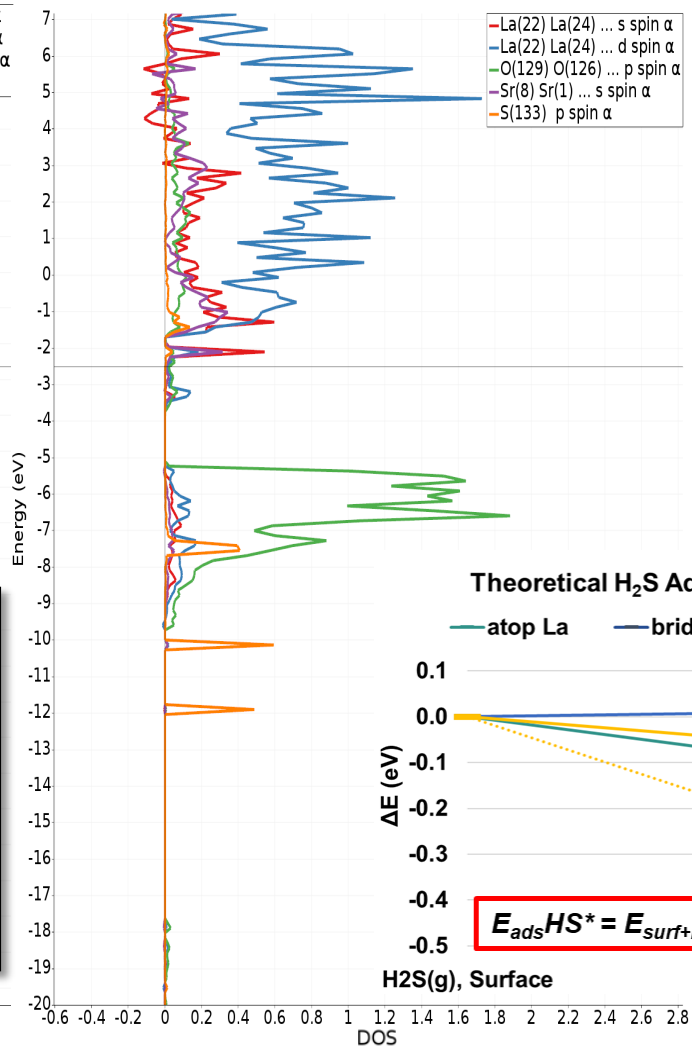

DFT - GGA:PBE:TZP:SFC:Normal

O: [He] $2s^2 2p^4$
V: [Ar] $4s^2 3d^3$
La: [Xe] $6s^2 5d^1$
Sr: [Kr] $5s^2$

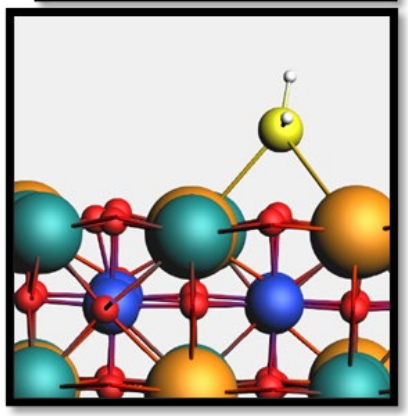

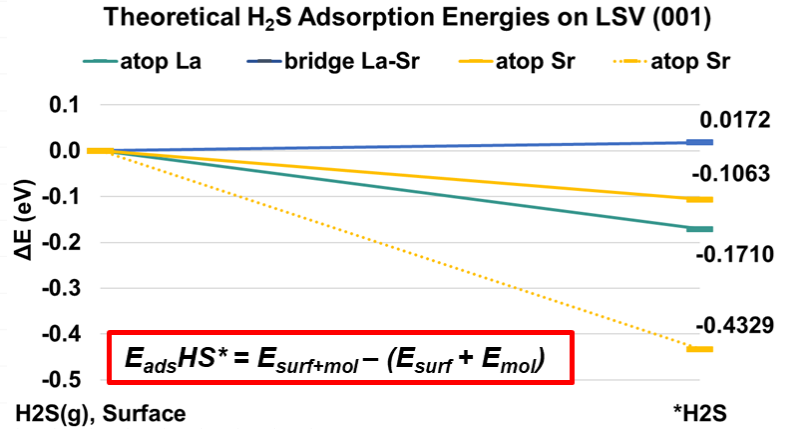

$LSV_{reduced}/H_2S$ Adsorption Study

Adsorption Products on V/O Termination

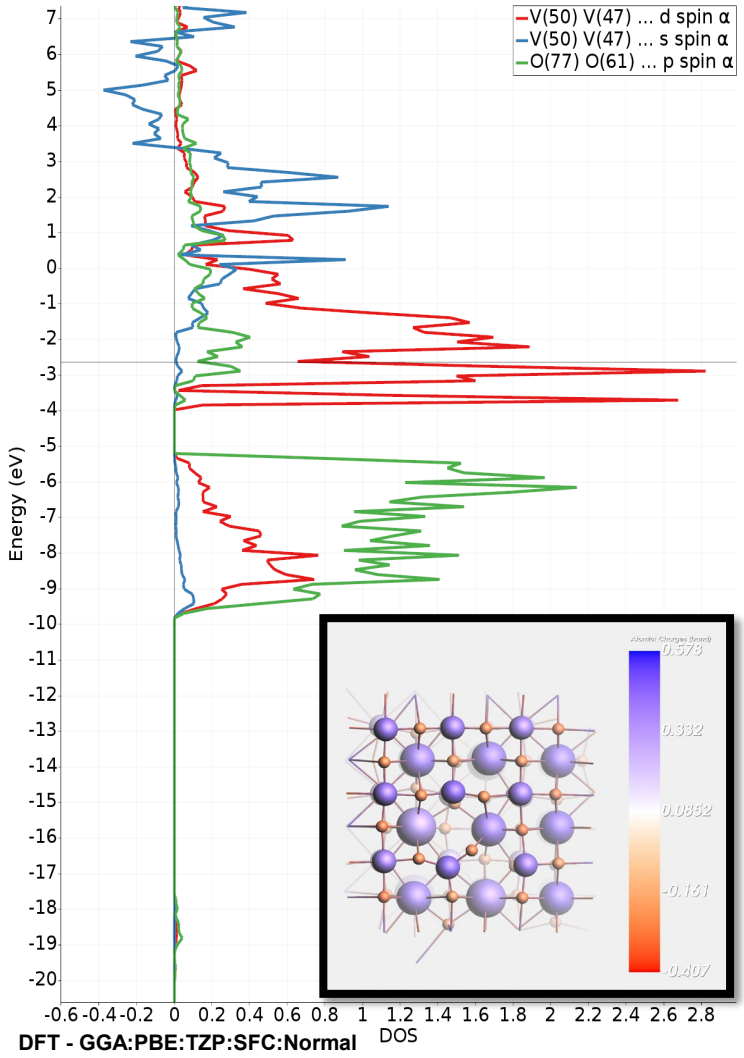

DFT - GGA:PBE:TZP:SFC:Normal

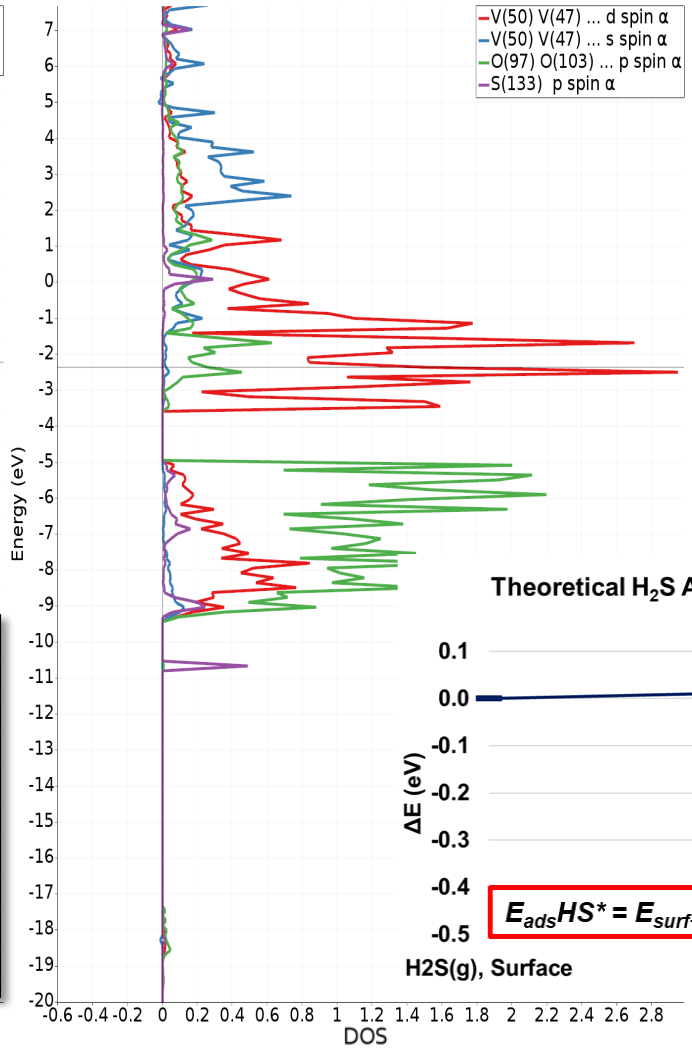

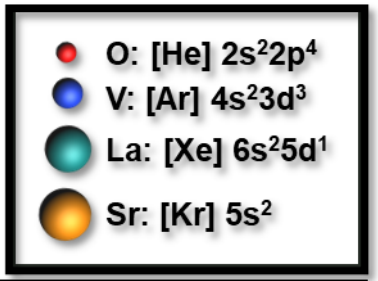

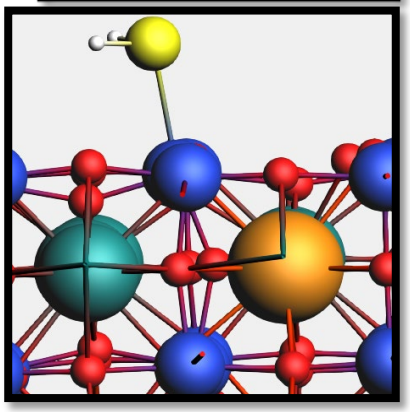

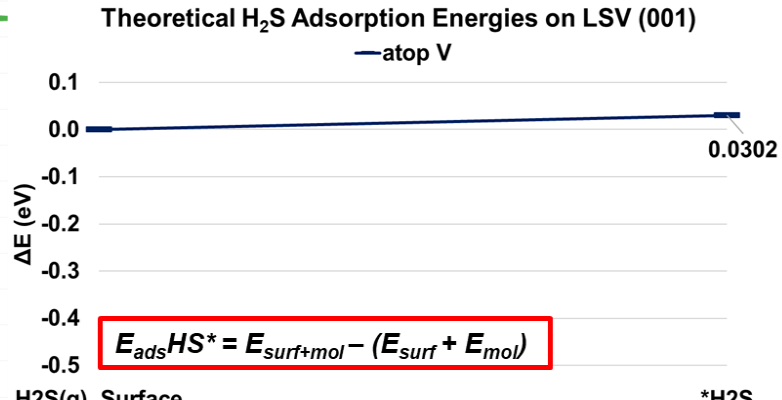

$LSV_{oxidized}/H_2S$ Adsorption Study

Adsorption Products on La/Sr Termination

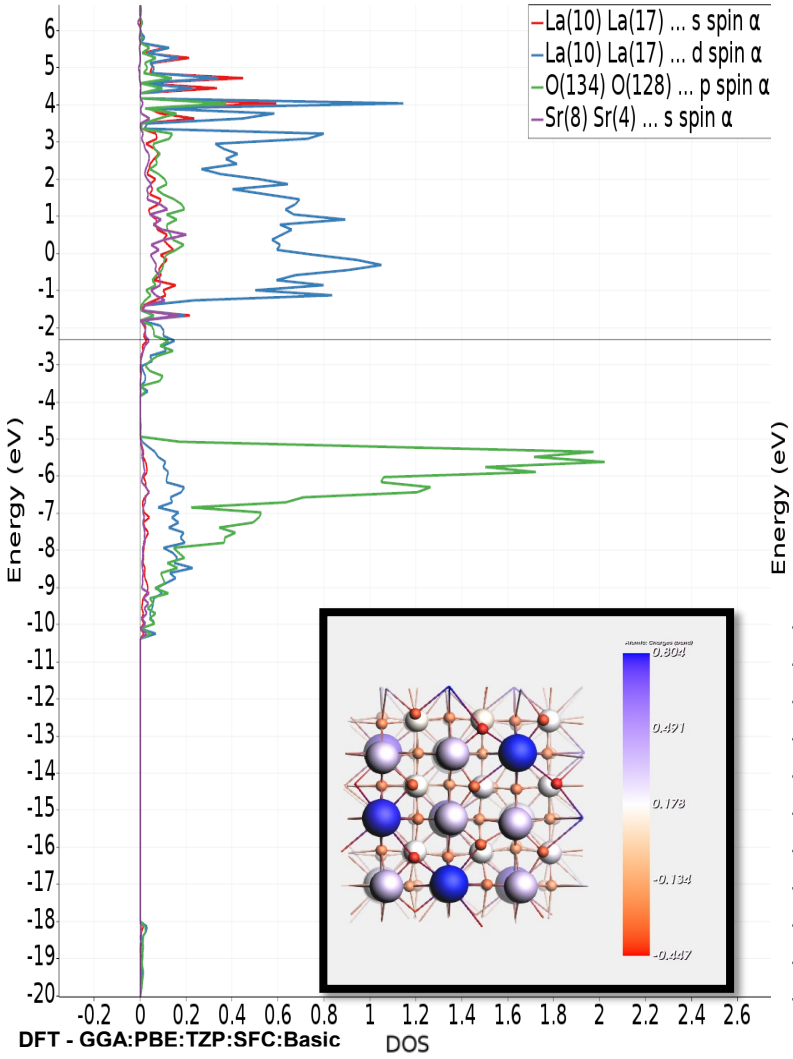

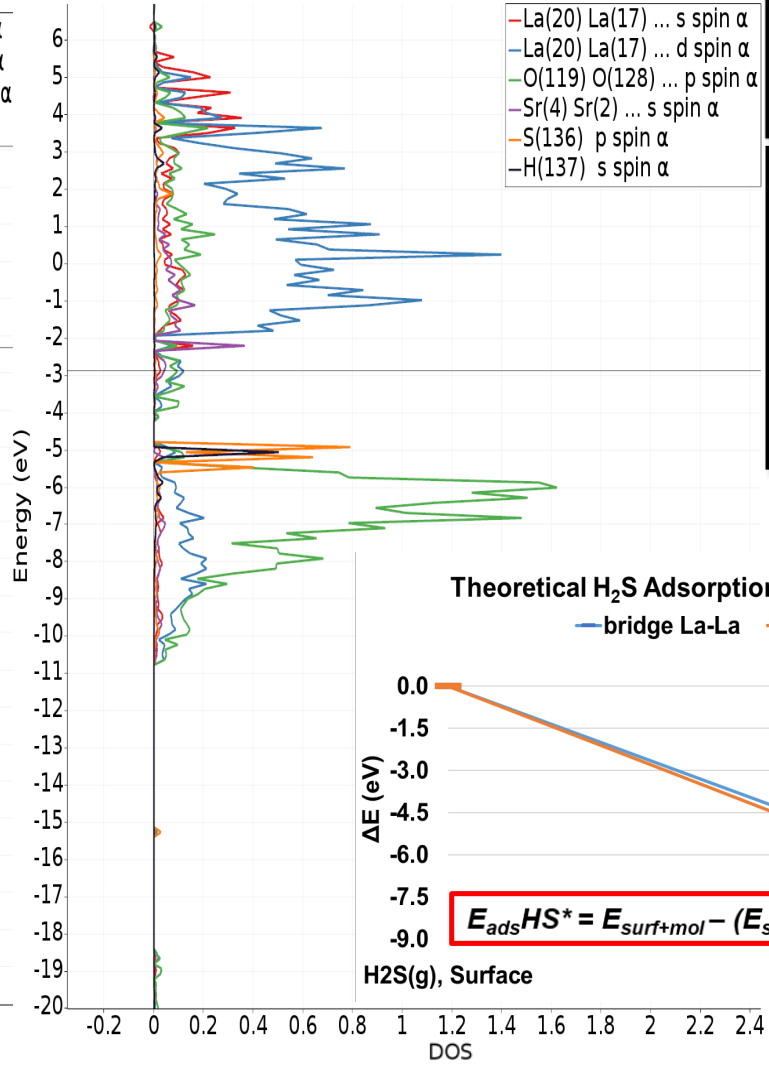

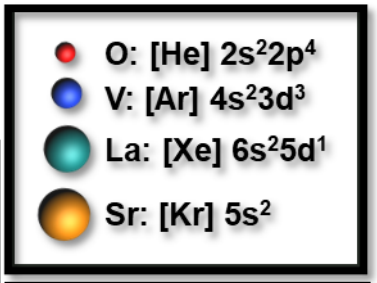

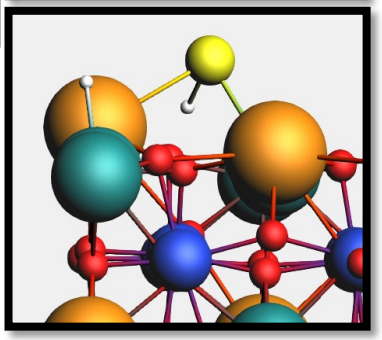

$LSV_{oxidized}/H_2S$ Adsorption Study

Adsorption Products on V/O Termination

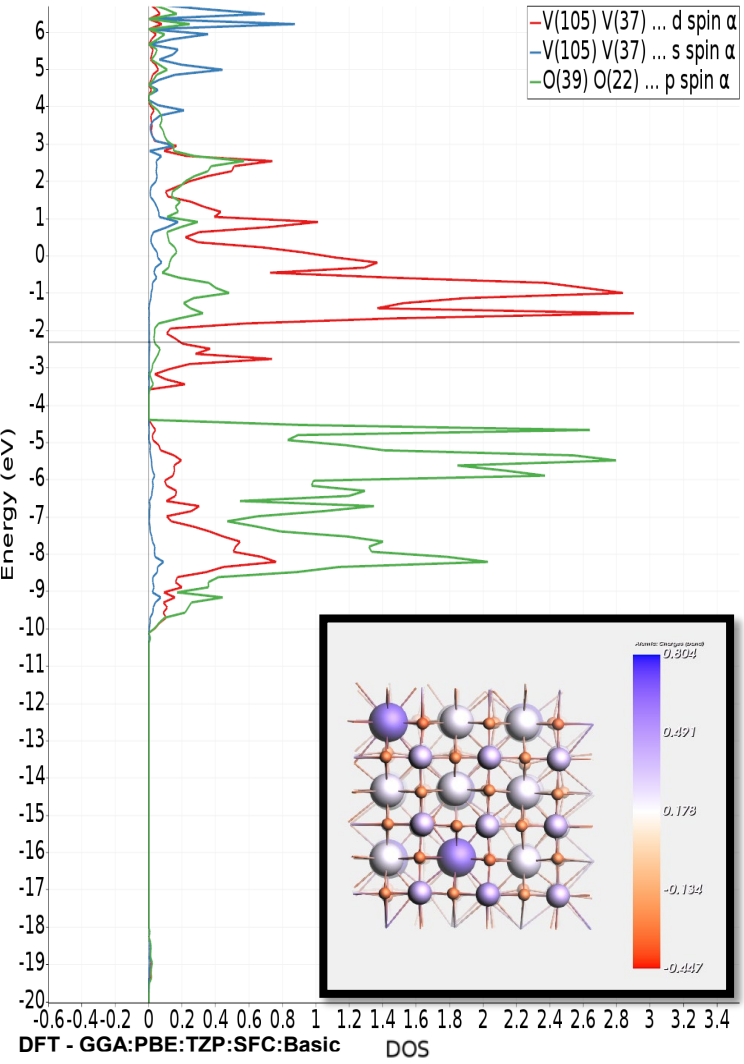

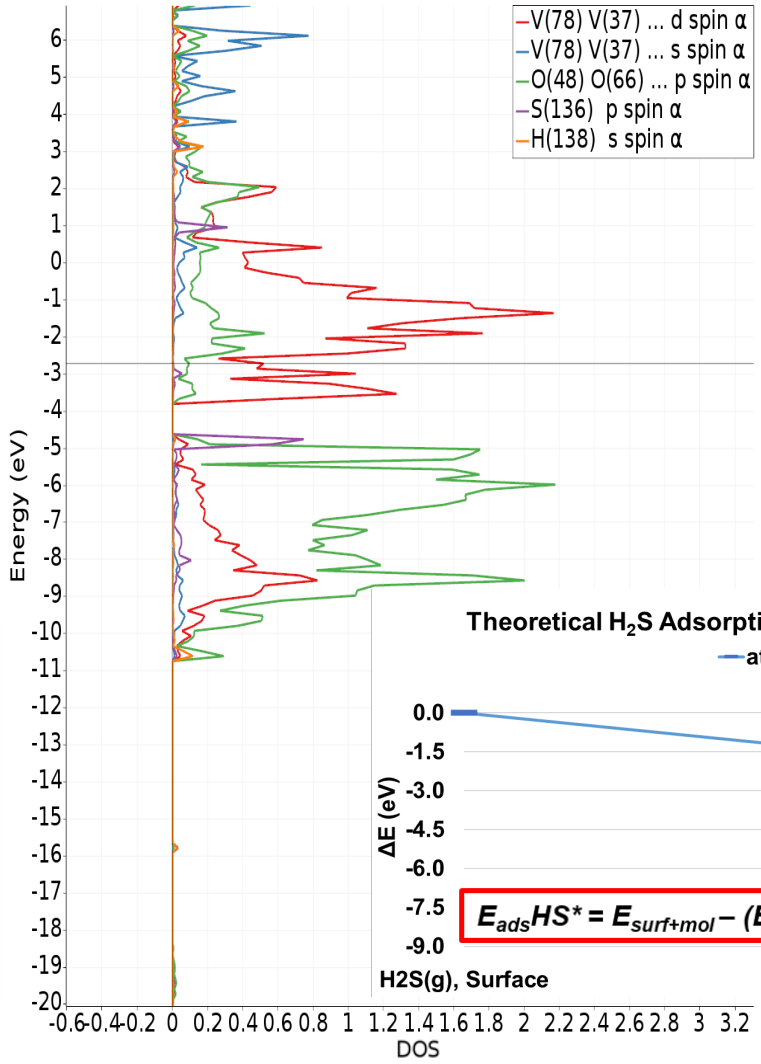

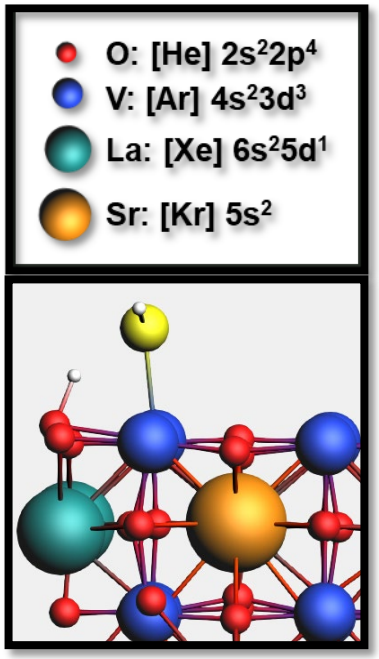

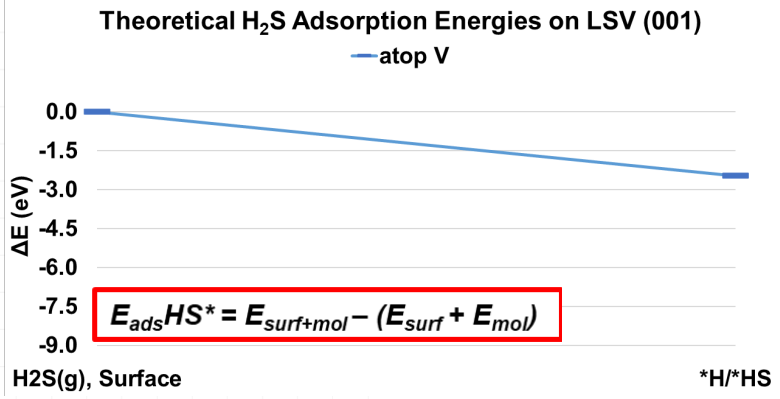

Conclusions

Experimental Results Conclusions

1. LSV adsorbs sulfur at a significantly lower rate than currently used Ni-YSZ
   - 278-287x lower (30-300ppm)

2. LSV in H_2 and CH_4 appears to have similar adsorption rates at low sulfur conc.
   - Adsorption may be different at higher sulfur concentration.

3. LSV sulfur adsorption rate significantly reduced/lowest at temperatures >500C
   - Cubic crystal structure hinders adsorption

4. CH_4 stabilizes monoclinic/tetragonal phases at higher temperatures (Undesirable)

Modeling Results Conclusions

- H_2S adsorbs primarily as molecular species on reduced LSV surfaces, near strontium impurities, likely due to polarity of surface near strontium, with low affinity for vanadium due to reduced state of vanadium ions.
- H_2S adsorption results primarily in single dissociated species on oxidized LSV surfaces, stronger reactions on La/Sr termination than V terminations.

Acknowledgements

Office of the Chief Scientist, GVSC

Fuel Cell Technologies Branch, GVSC

Fuels and Lubricants Branch, GVSC

Water Treatment and Handling Branch, GVSC

Characterization and Failure Analysis Branch, GVSC

Backup Slides

Experimental Results – Adsorption Rate Calculation

$$R_{ads} = \frac{Mass_{sulf,norm}}{\text{Time}_{duration}}$$

$$Mass_{sulf,norm} = \frac{Mass_{sulf}}{SA}$$

$$Time_{duration} = Gas\ Exposure\ Time\ (hrs)$$

$$Mass_{sulf} = Sulfur\ Mass\ (ng) \leftarrow \textbf{EDS}$$

$$\textbf{SA} = Surface\ Area\ (\mu m^2) \leftarrow \textbf{SEM}$$

- EDS Provides Weight % Sulfur - Convert to Sulfur Mass
- SEM Provides Agglomerate Size - Determine Surface Area

Backup Slides – Ni-YSZ EDS

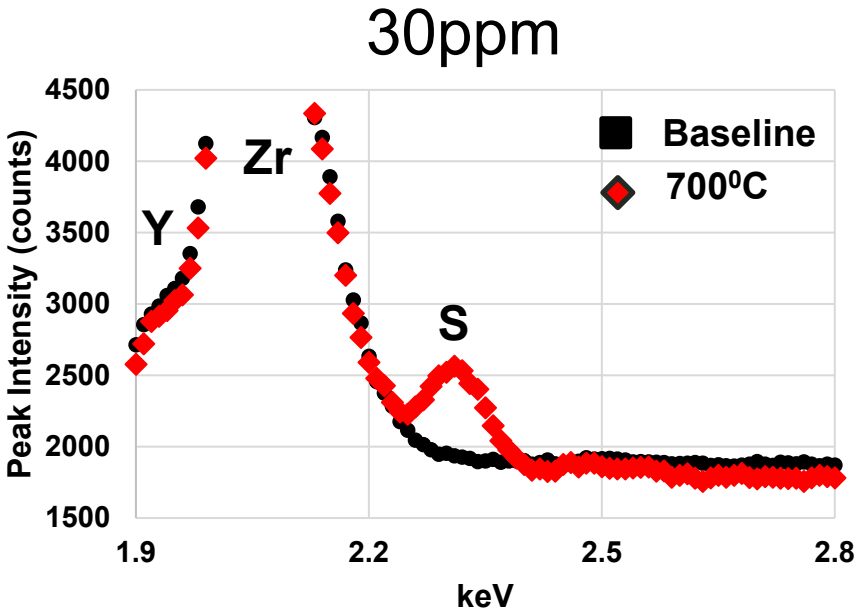

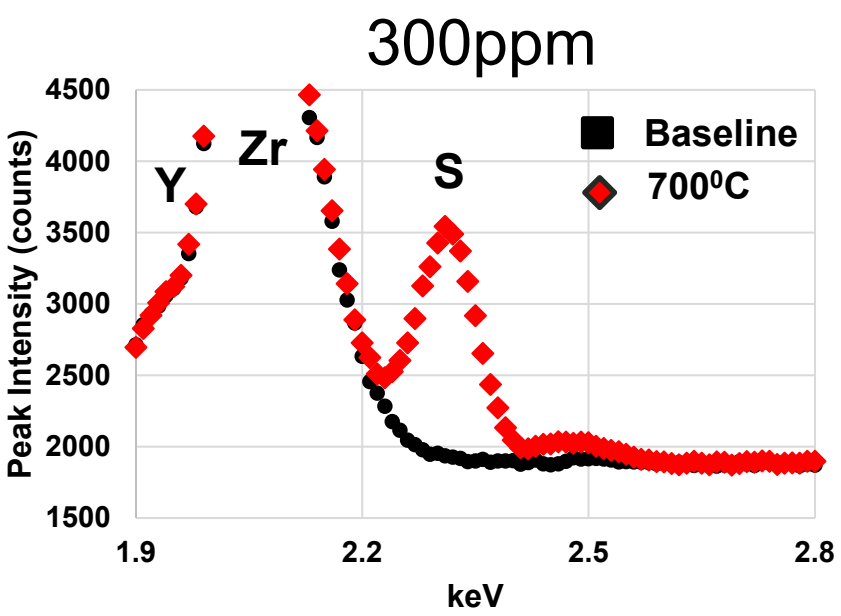

Experimental Results – SEM Images

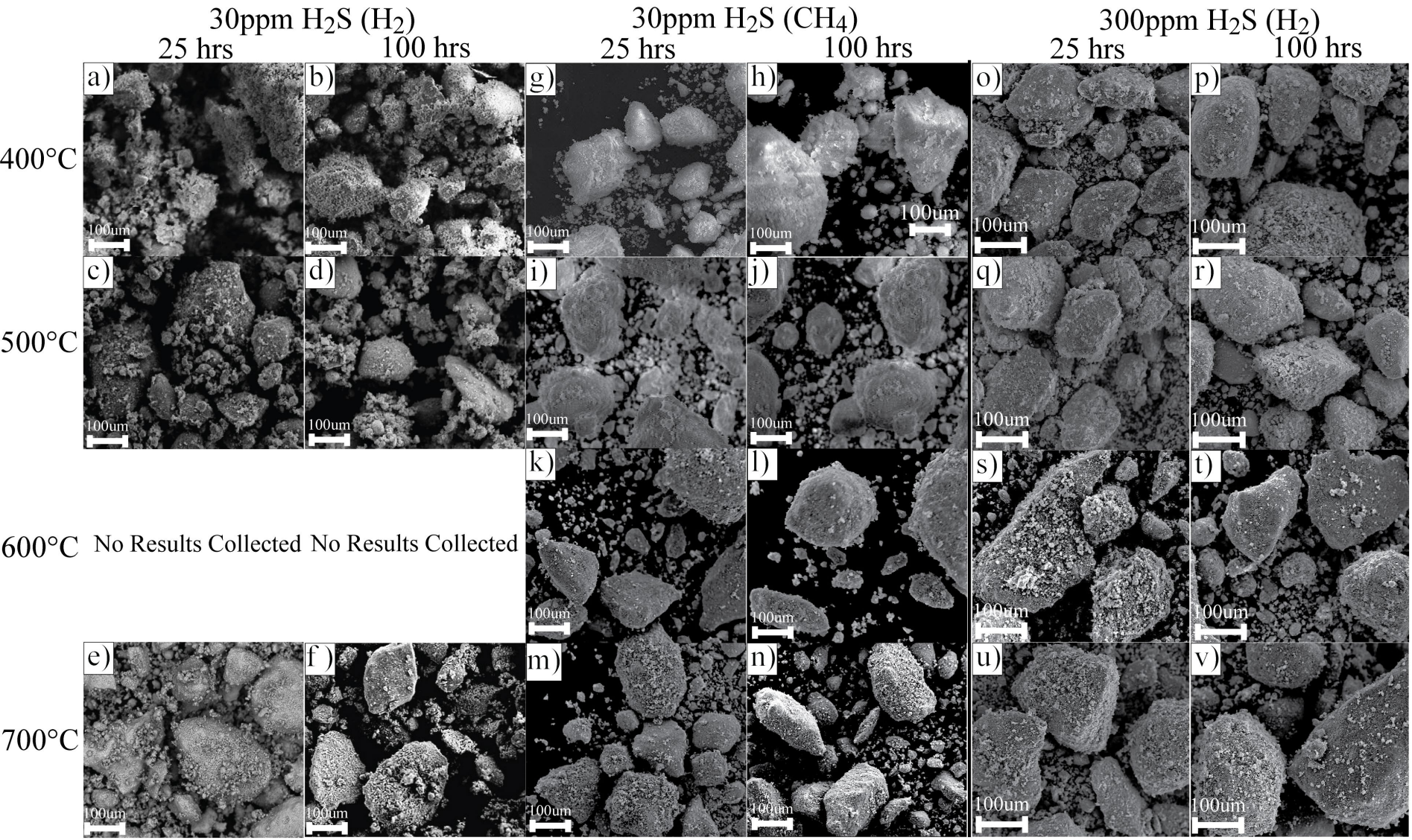

Backup Slides– LSV Optical Microscopy

La = +3 Sr = +2

Untested LSV Oxide Powder

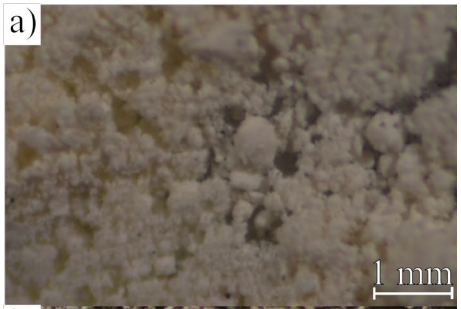

Cream

V = +5

30ppm H_2S 400°C LSV Oxide

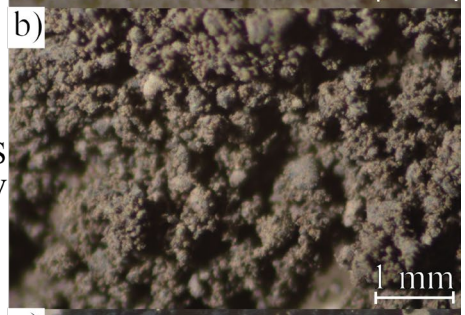

Brown/Yellow

V = +5

30ppm H_2S 500°C LSV Oxide

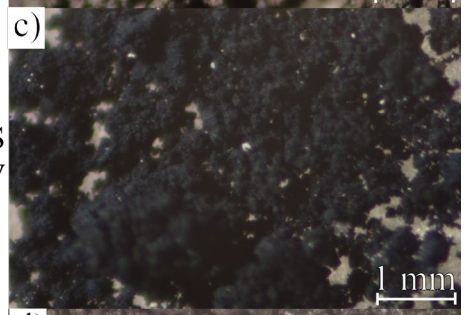

Dark Blue

V = +4

30ppm H_2S 700°C LSV Oxide

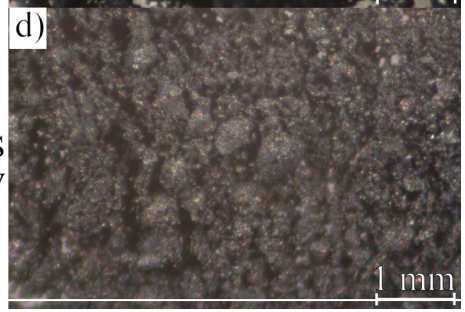

Black

V = +3

Backup Slides – Activation Energy Calculation

$$R_{ads,act} = k * P^{x}_{gas,partial}$$

$$P_{gas,partial} = P_{gas} * X_{H_2S}$$

$$\mathrm{X} = kinetic\ order\ (assume\ 1)$$

$$\mathrm{k} = kinetic\ rate\ constant$$

$$X_{H_2S} = H_2S\ Mol\ Fraction$$

$$P_{gas} = Gas\ Pressure\ on\ Sample\ (45\ PSI)$$

- Experimental and Kinetic Model Adsorption Rate Assumed Equal
- Kinetic Rate Constant Fitted to Match Experimental Adsorption Rate
  - Rate Constant Used to Determine Activation Energy

Backup Slides – Activation Energy Calculation

$$k = A * e^{\frac{-E_a}{R*T}} \rightarrow Ln(k) = \frac{-E_a}{R*T} + Ln(A)$$

R = Ideal Gas Constant

T = Temperature

E_a = Activation Energy (AE) (Energy Barrier for Reaction to Occur)

A = Pre-Exponential Factor (PEF) (Frequency of Collisions)

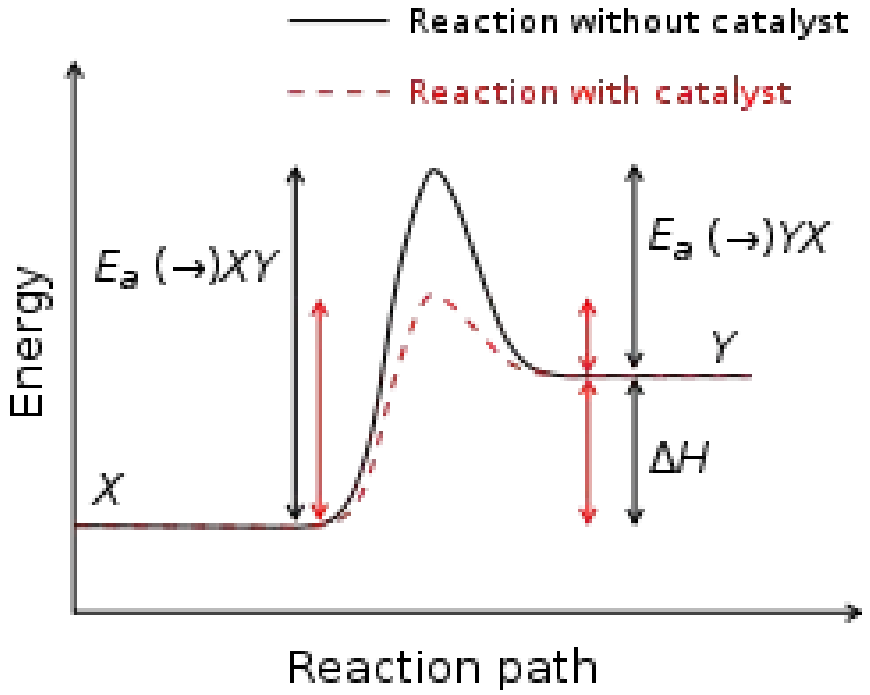

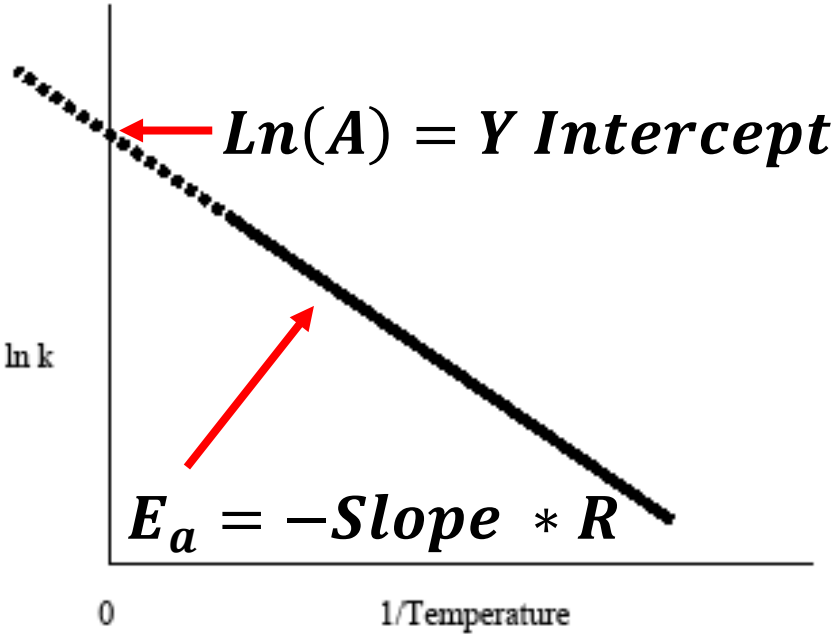

Backup Slides – Negative Activation Energy

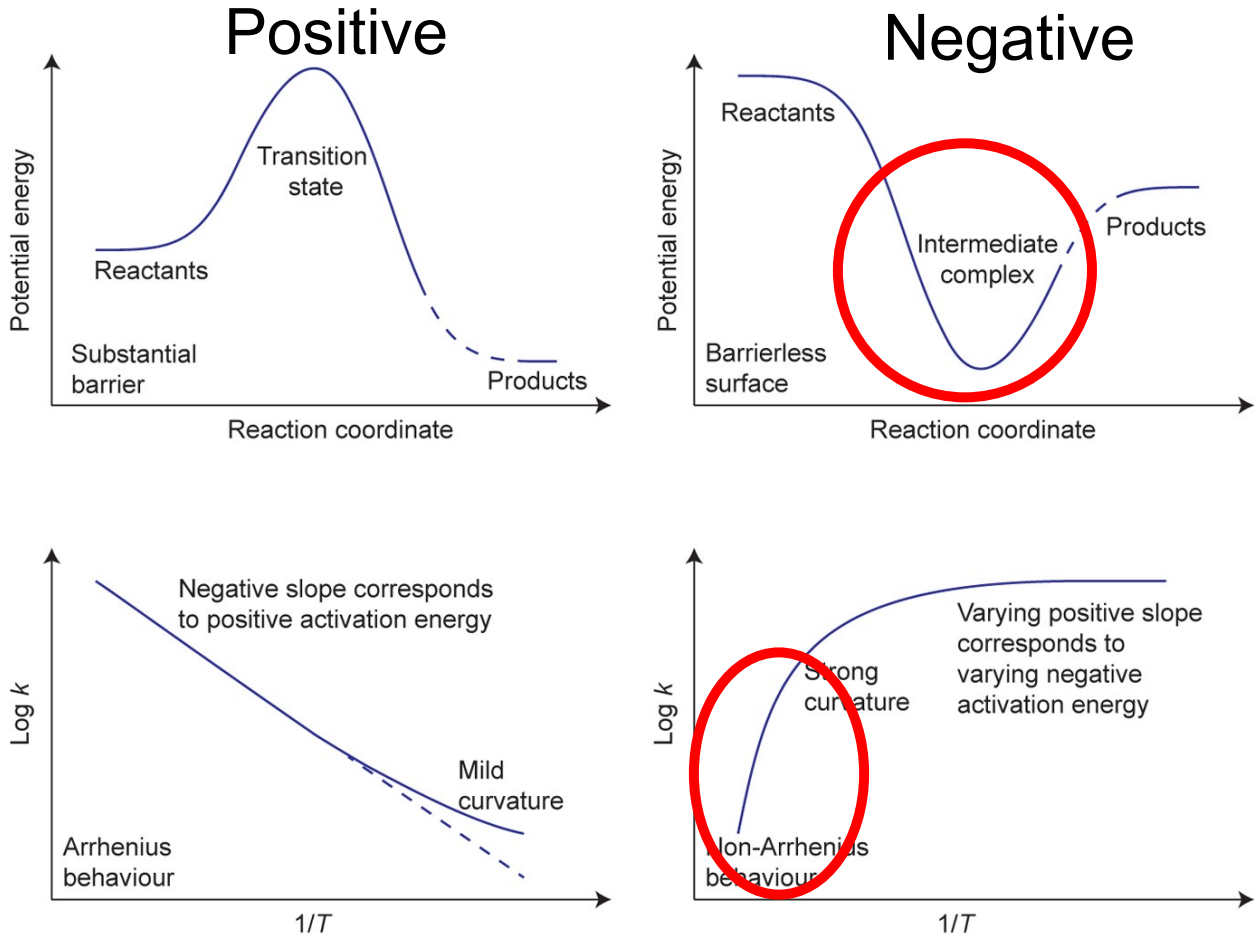

- Negative Activation Energy
  - Barrierless Reaction
  - Capture of Molecules in a Potential Well
  - Higher Temperature Drives more Molecules from Well
  - Less Negative Value has Greater Reaction Barrier

Future Material Tuning

Predictive Doping

n-dopants

	probability	dopant_species	original_species
0	0.066927	F-	O2-
1	0.021187	Re5+	V3+
2	0.021023	Cl-	O2-
3	0.011895	Zr4+	V3+
4	0.011134	Se4+	La3+
5	0.008980	Ti4+	V3+
6	0.007980	Ta5+	V3+
7	0.007413	W6+	V3+
8	0.007410	Mo6+	V3+
9	0.006920	Sn4+	V3+

p-dopants

	probability	dopant_species	original_species
0	0.092325	Sr2+	La3+
1	0.055816	Na+	V3+
2	0.047683	Ba2+	La3+
3	0.047199	Na+	La3+
4	0.035980	Ca2+	La3+
5	0.035979	K+	La3+
6	0.035651	Rb+	V3+
7	0.032114	Cs+	La3+
8	0.029616	K+	V3+
9	0.029187	Rb+	La3+

TGA Hydrogen Concentration Results

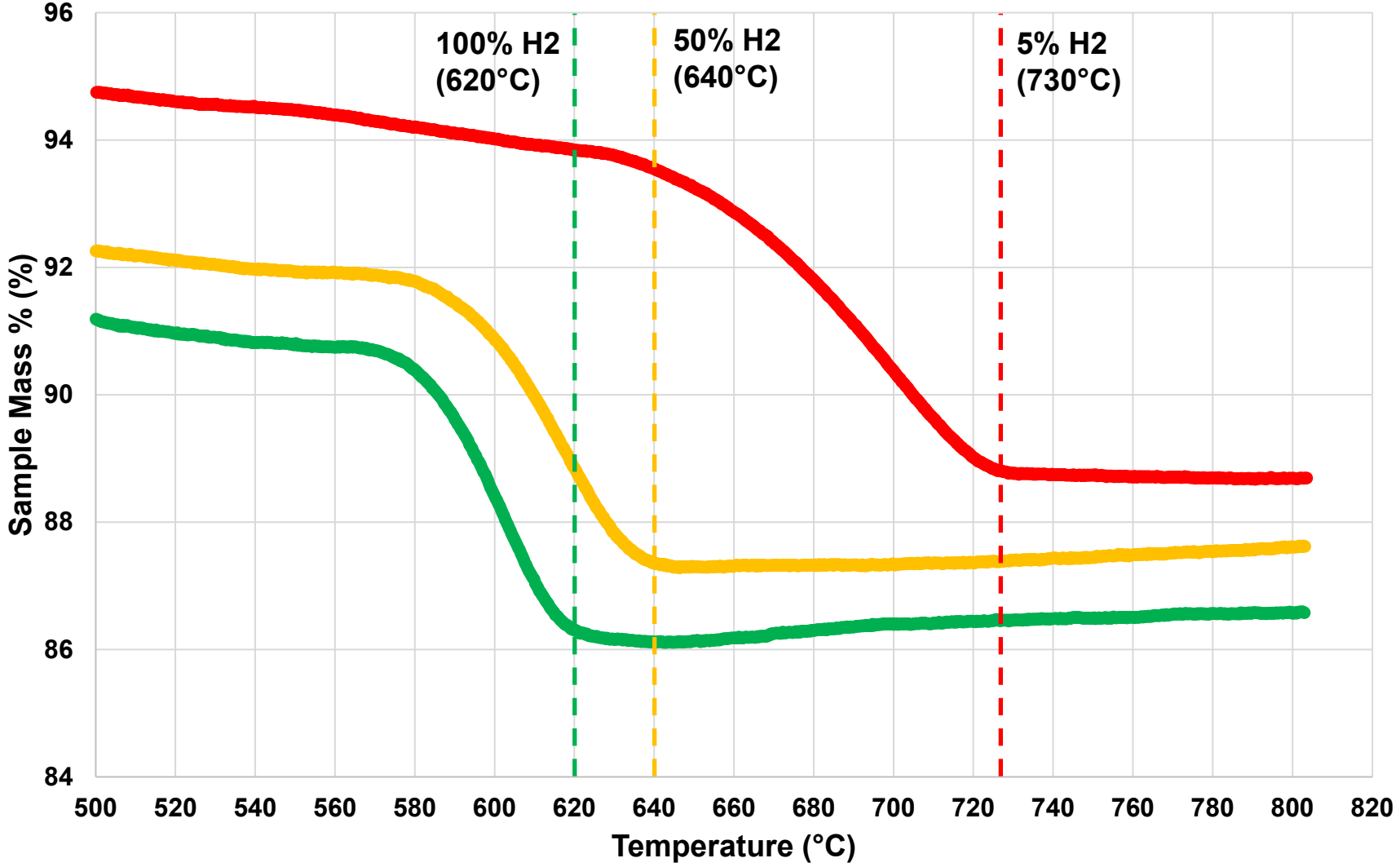

Current Surface Efforts

Non-polar and Symmetric Surfaces

- More accurate prediction of surface energy